R-Matrix study of electron impact excitation and dissociation of CH^+ ions

K. Chakrabarti[*], A. Dora[♯], R. Ghosh[‡], B. S. Choudhury[‡] and Jonathan Tennyson[†]

[*] Department of Mathematics, Scottish Church College, 1 & 3 Urquhart Sq., Kolkata 700006, India

[♯] Department of Chemistry, North Orissa University, Baripada 757003, Odisha, India

[‡] Department of Mathematics, Indian Institute of Engineering Science and Technology, Shibpur, Howrah 711103, India

[†] Department of Physics and Astronomy, University College London, Gower St., London WC1E 6BT, UK

E-mail: j.tennyson@ucl.ac.uk

Abstract. Electron impact excitation and electron impact dissociation of CH^+ ions are studied in the framework of the *R*-matrix method using the diatomic version of the UK molecular *R*-matrix codes. A configuration-interaction calculation is first performed to yield the potential energy curves of the lowest eight singlet and triplet states of CH^+. Scattering calculations are then performed to yield vibrationally-resolved electronic excitations to the lowest three bound states, namely the a $^3\Pi$, A $^1\Pi$ and the b $^3\Sigma^-$. Electron impact dissociation cross sections are obtained from the assumption that all electronic excitations above the dissociation threshold result in dissociation. Bound states of CH and resonance positions and widths of Feshbach resonances in the e-CH^+ system are also calculated at the CH^+ equilibrium bond length 2.137 a_0.

1. Introduction

Molecular ions are a constituent of many low temperature plasmas and diffuse interstellar clouds, where collision of these ions with electrons play an important role governing their chemistry. Hydrocarbon ions, and in particular CH^+, are found in the edge plasmas in those fusion reactors operating with graphite as plasma facing material (Tawara 1995). CH^+ ions also occur in the interstellar medium (ISM) where they were first detected and studied by Douglas & Herzberg (1941) in interstellar molecular clouds (see also Douglas & Herzberg (1942)).

Electron collision with CH^+ ions can lead to electronic excitation,

$$e^- + CH^+ \longrightarrow CH^{+*} + e^- \tag{1}$$

where CH^{+*} refers to an excited state of the ion, or destruction of the ion either by dissociation,

$$\begin{aligned} e^- + CH^+ &\longrightarrow C + H^+ + e^- \\ &\longrightarrow C^+ + H + e^- \end{aligned} \tag{2}$$

or by dissociative recombination via an intermediate neutral resonant state CH^{**},

$$e^- + CH^+ \longrightarrow CH^{**} \longrightarrow C + H. \tag{3}$$

Collision cross sections for these processes are therefore important for modeling of the plasma environment and to understand the chemistry of formation and destruction of CH^+ in the ISM (Godard *et al* 2012, Nagy *et al* 2013). There has been a long-running issue that the observed ISM concentration of CH^+ is persistently larger than that predicted by models (Hayden Smith *et al* 1973), see also Godard & Cernicharo (2013), Myers *et al* (2015) and references therein. This issue has recently been considered at length by Faure *et al* (2017) who showed that the proper treatment of non-local thermodynamic equilibrium effects are essential to model the production of CH^+ ions in the ISM.

Several earlier works on the CH^+ states have been undertaken of which we report only a few. Lorquet *et al* (1971) calculated the potential energy curves of CH^+ and studied its metastable decomposition and predissociation. Molecular constants including Franck-Condon factors for A $^1\Pi - $ X $^1\Sigma^+$ transitions were calculated by Liszt & Hayden Smith (1972) and Hakalla *et al* (2006). Tennyson (1988) reported the lowest three bound states of CH^+ while obtaining the bound states of CH and resonances in the e^- CH^+ system. Kanzler *et al* (1991) obtained the lowest seven CH^+ states of singlet and triplet symmetry. They also gave the dipole moments, transition moments, oscillator strengths and radiative lifetimes computed by quasi-degenerate many body perturbation theory. Better calculations were performed by Kowalski & Piecuch (2001) and Barinvos & van Hemert (2004) though both were restricted to the singlet states only. Sauer & Špirko (2013) obtained potential energy curves of the ground and several excited states of CH^+ which reproduced available spectroscopic data with high accuracy. More recently, a comprehensive set of CH^+ curves of singlet, triplet and quintet symmetries were obtained by Biglari *et al* (2014) using the multi-reference conguration interaction (MRCI) method with large basis sets. They also obtained transition dipole moments which were then used to calculate average lifetimes of excited state vibrational levels. Empirical potential energy curves for the X $^1\Sigma^+$ and A $^1\Pi$ states were obtained by Cho & Le Roy (2016) using an analysis of all available spectroscopic and photodissociation data; nuclear motion calculations using these curves reproduced all data within their range of uncertainties.

On the collisional aspects, photodissociation studies on CH^+ were reported by Barinvos & van Hemert (2004) and Boukaline *et al* (2005). Electron impact rotational excitation and de-excitation was reported by Lim *et al* (1999) using the *R*-matrix method. A second *R*-matrix calculation for rotational excitation of CH^+, together

with HeH$^+$ and ArH$^+$ was reported by Hamilton *et al* (2016) where they claimed an improvement of the rate coefficients for CH$^+$ over those of Lim *et al* (1999).

Some theoretical and experimental studies on the dissociative recombination and of rotational excitation of CH$^+$ also exist. A Multi Channel Quantum Defect Theory (MQDT) study of dissociative recombination of CH$^+$ and its isotopologue CD$^+$ was reported by Carata *et al* (2000) which were not in very good quantitative agreement with an earlier experimental study reported by Amitay *et al* (1996). Bannister *et al* (2003) reported an experimental study of the electron impact dissociation of CH$^+$ to the asymptotic states C$^+$(^2P) + H(^2S). They measured absolute cross sections for electron impact dissociation of CH$^+$ ions producing C$^+$ ions. However, as discussed below, the initial distribution of CH$^+$ ions in these experiments, in which neither the vibrational nor electronic states of the ions involved were well-characterised, makes these results hard to use in plasma models.

In this article, we present electron impact excitation cross sections of CH$^+$ to some of its low-lying states and cross sections for electron impact dissociation to the lowest C$^+$(^2P) + H(^2S) and C(^3P) + H$^+$ asymptotes. To the best of our knowledge, there exist no previous *ab initio* theoretical study on these aspects.

2. Calculations

2.1. Method

Our calculations are done using the *R*-matrix method, see reviews by Burke (2011) and Tennyson (2010). The starting point of such a calculation is the division of the configuration space into an inner region, here a sphere of radius 11 a$_0$, centred at the molecular centre-of-mass, which encloses the N-electron target CH$^+$ ion.

In the inner region, the wave function of the (N+1)-electron system (CH$^+$ + e^-) is written as a close coupling (CC) expansion,

$$\Psi_k = \mathcal{A}\sum_{i,j} a_{i,j,k}\Phi_i(1,\ldots,N)F_{i,j}(N+1) + \sum_i b_{i,k}\chi_i(1,\ldots,N+1)\,, \qquad (4)$$

where $\mathcal{A}$ is the antisymmetrisation operator, Φ_i is the n-electron wave function of the i^{th} target state, $F_{i,j}$ are continuum orbitals and χ_i are two-centre L^2 functions constructed by making all $(N+1)$-electrons occupy the target molecular orbitals (MOs), and takes into account the polarization of the N-electron target wave function in presence of the projectile electron.

Once a suitable target model is fixed, several scattering models can be constructed by choosing different expansions for the target wave function Φ_i. Simple approximations, for example, static exchange (SE) and static exchange with polarization (SEP) models use only the target ground state represented by a Hartree-Fock (HF) self consistent field (SCF) wave function. Using the SE model, one can represent only shape resonances, while Feshbach resonances can be described with the SEP models, though these are not well represented without the inclusion of their parent electronic states. More

sophisticated models, like the CC model used here, can include several target states and therefore are very suitable for representing Feshbach resonances and calculating electron impact cross sections.

The inner region wave function is used to build an R-matrix at the boundary of the R-matrix sphere and the R-matrix is then propagated to asymptotic distances and matched with known asymptotic functions (Noble & Nesbet 1984). The matching yields the K-matrix from which all scattering observables can be extracted.

For diatomic targets Slater type orbitals (STOs) are known to provide a better target representation. Hence the diatomic version of the UK molecular R-matrix codes (Morgan *et al* 1998) which uses STOs were used. The continuum (Tennyson & Morgan 1999) was represented by numerical orbitals in a partial wave expansion about the molecular centre of mass. These numerical orbitals were obtained as a solution of the radial Schrödinger equation with an isotropic Coulomb potential. A Buttle correction (Buttle 1967) was also used to allow for the arbitrary fixed boundary conditions imposed on the continuum basis orbitals.

2.2. CH$^+$ target calcultions

We have used the STOs of Cade & Huo (1967) which consisted of 5 s-type, 4 p-type, 2 d -type and 1 f-type STOs centered on the C atom and, 3 s-type and 1 p-type STOs centered on the H atom. These STOs were used to build a basis of 28 molecular orbitals comprising of 16 σ, 8 π, 3 δ and 1 ϕ orbitals. These were then used in an initial SCF calculation on the X $^1\Sigma^+$ state of CH$^+$. Finally, 16 σ, 8 π and 3 δ SCF orbitals were used in a complete active space (CAS) configuration interaction (CI) calculation.

We have tested different target models, a summary of which is presented in Table 1. Finally, target model 5 with an extended $(1\sigma)^2(2-8\sigma, 1-3\pi, 1\delta)^4$ CAS was chosen as it gave the best agreement in terms of excitation energies and dipole moments with the coupled cluster singles doubles and triples (CCSDT) calculations of Kowalski & Piecuch (2001) and the multi reference configuration interaction (MRCI) calculation of Biglari *et al* (2014). Figure 1 shows the behaviour of the lowest 9 CH$^+$ target potential energy curves (PECs). Shown also are the corresponding PECs obtained by Biglari *et al* (2014). In Figure 1 we have shifted the R-matrix curves down by 1.28 eV so that the two sets of curves have the same minima of the X $^1\Sigma^+$ ground state. We find general good agreement between the two sets of curves, though there are some deviations in the higher lying curves of b $^1\Delta$, c $^1\Sigma^+$ and the d $^1\Pi$ symmetries.

2.3. The scattering model

Our scattering calculations used 12 CH$^+$ SCF orbitals and a target CAS defined in Section 2.2. These were supplemented by continuum orbitals F_{ij} needed to describe the scattering electron. These were obtained as a truncated partial wave expansion around the centre of mass and partial waves with $l \leq 6$ and $m \leq 2$ were retained in the calculation as these range of values of l and m gave converged results with respect

Table 1. Comparison of the ground state energy (in Hartree), and excitation energies (in eV) from the ground states to 9 low lying states of CH^+ for different target models. Shown also are a comparison of the ground state dipole moment (in au). Absolute values of our dipole moments are presented since they differ in sign from those of Biglari *et al* (2014) due to differences in convention. The target models used are the following:
Model 1: $(1-6\sigma, 1-2\pi)^6$
Model 2: $(1\sigma)^2(2-6\sigma, 1-2\pi)^4$
Model 3: $(1\sigma)^2(2-8\sigma, 1-2\pi, 1\delta)^4$
Model 4: $(1\sigma)^2(2-6\sigma, 1-3\pi)^6$
Model 5: $(1\sigma)^2(2-8\sigma, 1-3\pi, 1\delta)^4$
Model 6: $(1\sigma)^2(2-10\sigma, 1-3\pi, 1\delta)^4$.

Target state	Model 1	Model 2	Model 3	Model 4	Model 5	Model 6	Theory
X $^1\Sigma^+$	-37.9626	-37.9623	-37.9755	-37.9689	-37.9816	-37.9912	-38.0196[a]
B $^1\Sigma^+$	8.79	8.79	8.84	8.52	8.57	8.70	8.549[a]
C $^1\Sigma^+$	15.03	15.03	14.75	14.91	14.63	14.61	13.525[a]
A $^1\Pi$	3.67	3.67	3.45	3.49	3.25	3.23	3.23[a]
B $^1\Pi$	14.66	14.66	14.17	14.60	14.10	14.15	14.127[a]
A $^1\Delta$	7.50	7.50	7.35	7.27	7.14	7.32	6.964[a]
B $^1\Delta$	17.88	17.88	17.08	17.40	16.64	16.71	16.833[a]
a $^3\Pi$	1.30	1.29	1.25	1.19	1.14	1.21	1.16496[b]
b $^3\Sigma^-$	5.18	5.18	5.13	4.96	4.89	5.05	4.64268[b]
Dipole moment	0.6227	0.7051	0.6860	0.6867	0.6308	0.6812	0.6501[a]

[a] Kowalski & Piecuch (2001)
[b] Biglari *et al* (2014)

to bound state energies and resonance positions. The radial Coulomb functions were generated as numerical solutions of an isotropic Coulomb potential and solutions with an energy below 10 Ryd were retained. An R-matrix radius of 11 a_0 was used and this produced 175 (70σ, 58π, 47δ) continuum functions which were Schmidt orthogonalised to the target SCF orbitals. Scattering calculations were then performed using the $(1\sigma)^2(2-8\sigma, 1-3\pi, 1\delta)^4$ CAS-CI target wave function for a single geometry, namely the CH^+ equilibrium geometry $R_e = 2.137$ a_0.

Extensive tests were made with different scattering models by varying the number and nature of the target states used. Our final scattering models for the different CH states, and the number and nature of the targets states used are shown in Table 2. These were chosen so as to give the lowest energy of X $^2\Pi$ ground state of CH and the best vertical excitation energies compared to existing works of van Dishoeck (1987), Song *et al* (2008) and experiments where available .

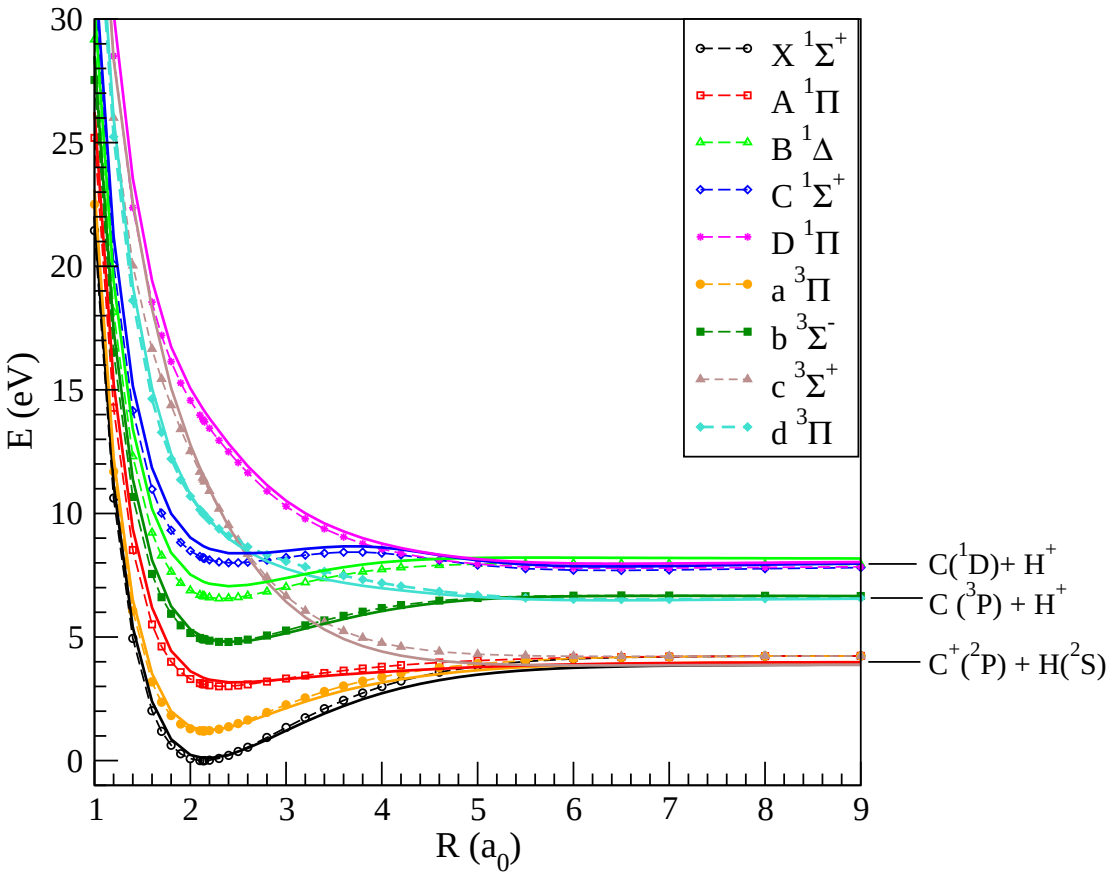

Figure 1. Potential energy curves of the CH^+ target states used in the calculation. Continuous curves: Present calculation shifted down by 1.28 eV. Dashed curves with symbols: Biglari *et al* (2014).

Table 2. Symmetry and number of states used in the close coupling equation 4. The target states of lowest energy were used in each case.

Symmetry	Number	Target states coupled
$^2\Pi$	8	two $^1\Sigma^+$, one each of $^1\Pi$, $^1\Delta$, $^3\Sigma^+$ $^3\Sigma^-$ and two $^3\Pi$
$^2\Sigma^+$	7	two $^1\Sigma^+$, one each of $^1\Pi$, $^1\Delta$, $^3\Sigma^+$ and two $^3\Pi$
$^2\Sigma^-$	5	one each of $^1\Sigma^-$, $^1\Pi$, $^1\Delta$ and two $^3\Pi$
$^2\Delta$	7	one each of $^1\Sigma^+$, $^1\Pi$, $^1\Delta$, $^3\Sigma^+$, $^3\Sigma^-$ and two $^3\Pi$
$^4\Pi$	5	one each of $^3\Sigma^+$, $^3\Sigma^-$, $^3\Delta$ and two $^3\Pi$
$^4\Sigma^+$	3	one $^3\Sigma^-$ and two $^3\Pi$
$^4\Delta$	4	one each of $^3\Sigma^+$, $^3\Sigma^-$ and two $^3\Pi$

3. Results

In this section we report our calculation for the bound states of CH, cross sections for electronic excitation from the CH$^+$ X $^1\Sigma^+$ ground state and electron impact dissociation at the CH$^+$ equilibrium geometry $R_e = 2.137$ a$_0$.

3.1. Bound states

An R-matrix was constructed at the boundary using the inner region solutions obtained as outlined above. In the outer region, the potential was given by the diagonal and off-diagonal dipole and quadrupole moments of the CH$^+$ target states in addition to the Coulomb potential. The outer region bound wave functions were propagated in this potential to 40 a$_0$ using the improved Runge-Kutta-Nystrom procedure implemented by Zhang *et al* (2011) to the asymptotic region, where they were matched with asymptotic solutions obtained from a Gailitis expansion (Noble & Nesbet 1984). Bound states were then found using the searching algorithm of Sarpal *et al* (1991) with the improved nonlinear, quantum defect based grid of Rabadán & Tennyson (1996). These calculations were performed at the CH equilibrium geometry $R_e = 2.116$ a$_0$ as this facilitates direct comparison with other studies.

Table 3 shows the vertical excitation energies from the CH X $^2\Pi$ ground state. Shown also are the results from van Dishoeck (1987), Song *et al* (2008) and the experimental values given by Herzberg & Johns (1969). Our excitations energies are within 0.2 eV of the corresponding energies of other reported calculations presented in the table.

The ionization potential (IP) of CH has been reported by some authors. For the X $^2\Pi$ ground state, Tennyson (1988) reported an ionization potential of 10.83 eV which agreed reasonably with the 10.64 eV measurement of Herzberg & Johns (1969). Our estimate for the ionization potential at $R_e = 2.116$ a$_0$ is about 10.43 eV and is 2% from the experimental value of Herzberg & Johns (1969).

3.2. Resonances

It is well known that in an adiabatic fixed nuclei calculation, diabatic neutral states lying in the continuum above the ion appear as resonances having finite widths that are inversely proportional to their lifetimes. These states play an important role in several collision processes such as vibrational excitation and dissociative recombination. Here we try to estimate the position and widths of the resonant states at a single geometry, $R_e = 2.137$ a$_0$.

For calculation of resonances, the R-matrix were propagated (Morgan 1984) to 70 a$_0$, as tests showed that this produced stable results. It was then matched with asymptotic Coulomb functions (Barnett 1982) obtained using the Gailitis expansion procedure of Noble & Nesbet (1984). Resonances were detected and fitted to a Breit-Wigner profile to obtain their energy (E) and width (Γ) using the RESON program

Table 3. Vertical excitation energies (in eV) from the X $^2\Pi$ ground states of the CH molecule at CH equilibrium bond lenght $R = 2.116$ a$_0$.

CH state	This work	van Dishoeck[a]	Song *et al* [b]	Experiment[c]
X $^2\Pi$	0.0	0.0	0.0	0.0
a $^4\Sigma^-$	0.60	0.71	0.67	0.74
A $^2\Delta$	3.04	3.00	2.91	2.88
B $^2\Sigma^-$	3.33	3.24	3.17	3.19
C $^2\Sigma^+$	4.06	4.02	3.89	3.94
2 $^2\Sigma^+$	6.42	6.39		
2 $^2\Pi$	7.52	7.43		7.31
3 $^2\Pi$	7.72*	7.94		7.96
3 $^2\Sigma^+$	7.92	7.96		8.00
1 $^4\Pi$	7.50	7.55		
4 $^2\Sigma^+$	8.59	8.63		
2 $^2\Delta$	8.87	8.93		9.05
4 $^2\Pi$	8.87	8.05		
2 $^4\Pi$	8.83	8.90		
2 $^2\Sigma^-$	9.04	9.06		
1 $^4\Delta$	9.05	9.10		
5 $^2\Pi$	9.13	9.04		
3 $^2\Delta$	9.36	9.39		

[a]van Dishoeck (1987)
[b]Song *et al* (2008)
[c]Herzberg & Johns (1969)
* Estimated from the corresponding R-matrix pole.

(Tennyson & Noble 1984) with an energy grid 0.5×10^{-3} Ryd. The magnitudes of the complex quantum defects $\mu = \alpha + i\beta$ were obtained using the relations (Tennyson 1988)

$$E_r = E_t - \frac{1}{\nu^2}, \quad \Gamma = \frac{2\beta}{\nu^3} \tag{5}$$

where the effective quantum number ν equals $n - \alpha$ and E_t is the energy of the threshold to which the Rydberg series converges.

Tables 4 and 5 shows some of the resonances, their widths and effective quantum numbers for CH at $R_e = 2.137$ a$_0$ for doublet and quartet states, respectively. The resonances are presented in terms their CH$^+$ parent electronic state. The effective quantum numbers are calculated assuming the resonances can be associated with this parent state. Many of the resonances in the tables are seen to form a series with respect to their effective quantum numbers. The behaviour of these resonance series and their widths are the starting point for the construction of dissociative states and electronic couplings that are the basis for dissociative recombination (Little *et al* 2014, Mezei *et al* 2016, Laporta *et al* 2017).

Table 4. Resonance positions and widths (in Ryd) and effective quantum numbers at $R = 2.137$ a$_0$ for some doublet states of the e^--CH$^+$ system below the first two CH$^+$ excited states. Numbers within brackets indicate power of 10.

Below a $^3\Pi$ state			Below A $^1\Pi$ state		
Position	Width	ν	Position	Width	ν
$^2\Pi$					
0.0134	0.6872(-03)	3.7743	0.0933	0.1333(-01)	2.6222
0.0199	0.3979(-04)	3.9639	0.1281	0.5984(-03)	3.0060
0.0317	0.1137(-02)	4.3889	0.1481	0.3994(-02)	3.3207
0.0383	0.1585(-03)	4.6973	0.1606	0.4663(-02)	3.5770
0.0430	0.2552(-04)	4.9626	0.1739	0.1945(-03)	3.9247
0.0464	0.4230(-03)	5.1885	0.1854	0.1790(-02)	4.3279
0.0514	0.1004(-03)	5.5727	0.1908	0.2025(-02)	4.5646
0.0600	0.2141(-03)	6.5166	0.1984	0.1376(-03)	4.9755
0.0619	0.2913(-03)	6.7941	0.2019	0.6828(-03)	5.2058
$^2\Sigma^-$					
0.0370	0.5528(-03)	2.9086	0.3324	0.6312(-03)	3.0324
0.0675	0.6537(-03)	3.3773	0.3796	0.1938(-03)	4.0312
0.0894	0.2046(-03)	3.8998	0.4015	0.1053(-03)	5.0267
0.1030	0.1655(-03)	4.3774	0.4136	0.6336(-04)	6.0237
0.1134	0.7511(-04)	4.8935			
0.1206	0.5528(-04)	5.3753			
0.1306	0.2767(-04)	6.3729			
0.1341	0.1847(-04)	6.8853			
$^2\Delta$					
0.0319	0.2427(-04)	4.4005	0.1044	0.1741(-01)	2.7280
0.0496	0.1137(-03)	5.4221	0.1382	0.2415(-01)	3.1527
0.0595	0.7277(-03)	6.4447	0.1465	0.2844(-04)	3.2913
0.0657	0.1682(-03)	7.4813	0.1666	0.5492(-05)	3.7212

3.3. Electron impact excitation

Figure 2 shows the vibrationally-resolved electronic-excitation cross sections from the X $^1\Sigma^+$ vibrational ground states to the a $^3\Pi$, A $^1\Pi$ and b $^3\Sigma^-$ excited states, the vibrational state ν' being indicated in each panel. To calculate the vibrationally resolved cross sections we first calculated Franck-Condon factors corresponding to the transitions from the a $^3\Pi$, A $^1\Pi$ and b $^3\Sigma^-$ states to the X $^1\Sigma^+$ state with the potential energy curves of Biglari *et al* (2014) using Le Roy's LEVEL program (Le Roy 2017), and these are presented in Table 6. At least for the A $^1\Pi \rightarrow X^1\Sigma^+$ transitions, these are in good agreement to within 10% of the Franck-Condon factors computed with more accurate potential energy curves (Hakalla *et al* 2006). We did not use the Franck-Condon factors computed with our CI curves of Figure 1 since these were not as accurate as the Franck-

Table 5. Resonance positions and widths (in Ryd) and effective quantum numbers at $R = 2.137$ a$_0$ for some quartet states of the e$-c$ H$^+$ system below the first two CH$^+$ excited states. Numbers within brackets indicate power of 10.

Below a $^3\Pi$ state			Below A $^1\Pi$ state		
Position	Width	ν	Position	Width	ν
$^4\Pi$					
0.0980	0.3412(-02)	2.3684	0.5263	0.4887(-01)	2.0909
0.1598	0.7635(-03)	2.9298	0.5917	0.7974(-02)	2.4744
0.1886	0.5668(-03)	3.3765	0.6399	0.1414(-02)	2.9467
0.2111	0.3134(-03)	3.9170	0.6704	0.2675(-02)	3.4371
0.2242	0.2237(-03)	4.3805	0.6900	0.5549(-03)	3.9192
0.2348	0.1597(-03)	4.9118	0.7036	0.8360(-03)	4.4093
0.2417	0.1132(-03)	5.3825	0.7135	0.2518(-03)	4.9069
0.2476	0.9161(-04)	5.9091	0.7207	0.3149(-03)	5.3900
$^4\Sigma^-$					
0.0840	0.6302(-02)	2.2806			
0.1363	0.5288(-02)	2.6726			
0.1600	0.5792(-03)	2.9325			
0.1848	0.1741(-02)	3.3074			
0.1999	0.1882(-02)	3.6195			
0.2118	0.2072(-03)	3.9399			
0.2225	0.7533(-03)	4.3142			
0.2291	0.8264(-03)	4.6022			
$^4\Delta$					
0.1665	0.7112(-04)	3.0178	0.5747	0.6877(-02)	2.3543
0.2137	0.5385(-04)	3.9987	0.6409	0.7390(-03)	2.9595
			0.6907	0.2092(-03)	3.9426
			0.7267	0.5190(-04)	5.9343

Condon factors of Biglari *et al* (2014) for the A $^1\Pi \rightarrow X^1\Sigma^+$ transitions.

To get the vibrationally resolved cross sections, subsequently the cross sections were scaled with the Franck-Condon factor corresponding to the $\Gamma(\nu' = j) \rightarrow X^1\Sigma^+(\nu'' = 0)$ transitions, where Γ is one of the excited states mentioned above and $j = 0, 1, 2$ or 3.

The cross sections show numerous oscillations due to the resonance structure associated with excited Rydberg states of CH. A full treatment of the vibrational motion would tend to smooth these out. Noteworthy is also the X $^1\Sigma^+(\nu'' = 0) \rightarrow$ a $^3\Pi(\nu' = 0)$ cross section, which is $2-3$ orders of magnitude higher than all others indicating that in the energy range considered almost all the electronic transitions are to the a $^3\Pi(\nu' = 0)$ state.

Table 6. Franck-Condon factors used to get the vibrationally resolved cross sections in Figure 2 using the curves of Biglari *et al* (2014). ν' and ν'' label the vibrational levels of the upper states and the X $^1\Sigma^+$ ground state respectively. The quantities in the brackets are the corresponding Franck-Condon factors of Hakalla *et al* (2006).

	$\nu'=0$	$\nu'=1$	$\nu'=2$	$\nu'=3$
A $^1\Pi - X^1\Sigma^+$				
$\nu''=0$	0.6066 (0.6343)	0.2644 (0.2580)	0.0845 (0.0769)	0.0259 (0.0217)
a $^3\Pi - X^1\Sigma^+$				
$\nu''=0$	0.9968	0.0031	0.0001	0.0
b $^3\Sigma^- - X^1\Sigma^+$				
$\nu''=0$	0.6205	0.2690	0.0808	0.0217

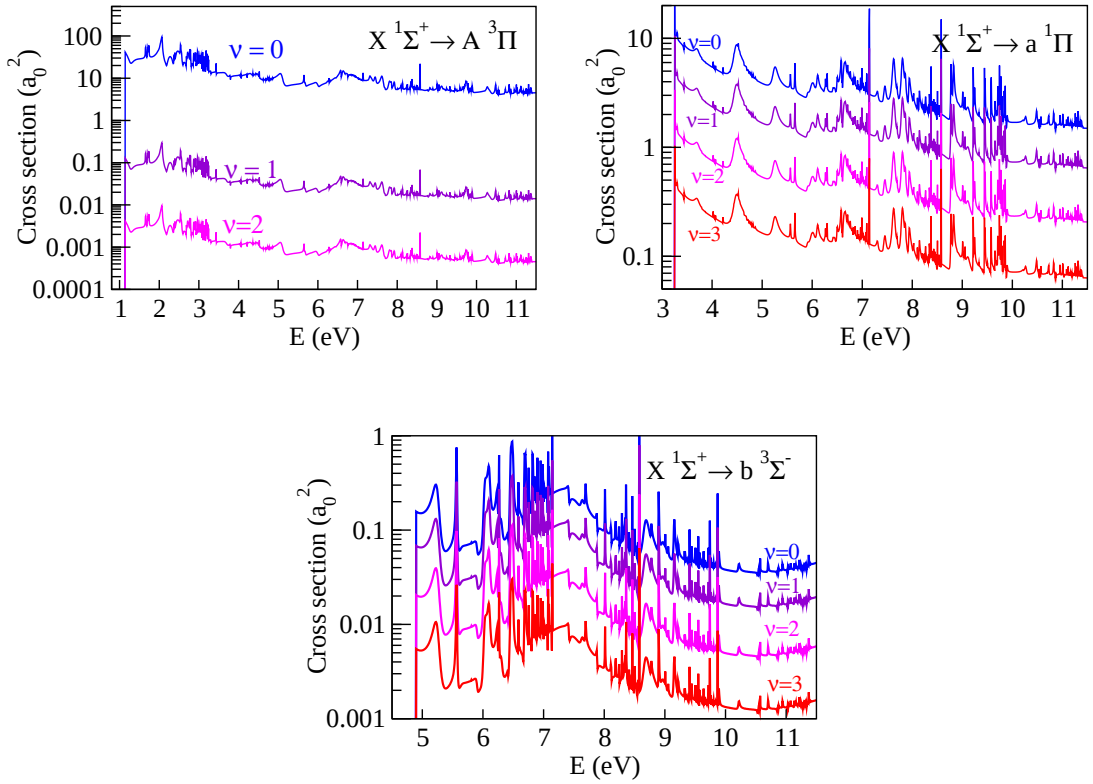

Figure 2. Excitation cross sections from the X $^1\Sigma^+$ ground state of the CH^+ molecule to the excited states with vibrational quantum number ν' as indicated in each panel at $R = 2.137$ a_0.

3.4. Electron impact dissociation

To the best of our knowledge, no theoretical calculation of the electron impact dissociation of CH^+ have ever been reported. Figure 1 shows the dissociation limits

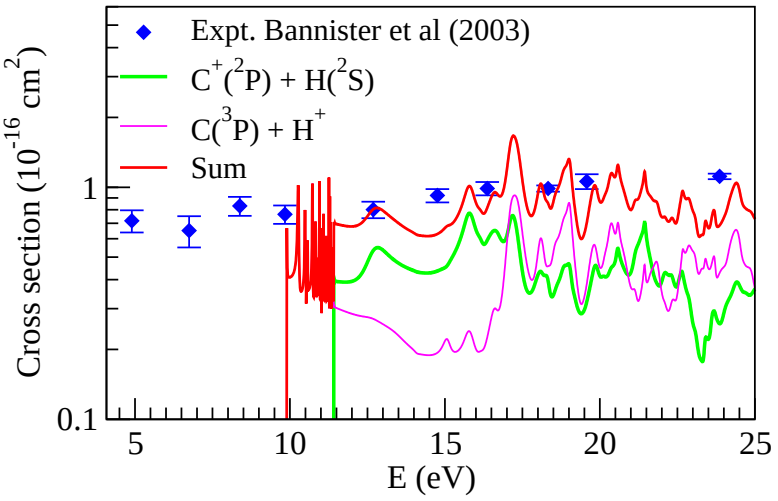

Figure 3. Electron impact dissociation of the CH^+ molecule Curves as indicated in the panel. Experiment: Bannister *et al* (2003).

for some the PECs included in this calculation. The X $^1\Sigma^+$, a $^3\Pi$, A $^1\Pi$ and c $^3\Sigma^+$ states dissociate to the fragments $C^+(^2P)$ + $H(^2S)$, while the b $^3\Sigma^-$ and d $^3\Pi$ states dissociate into the fragments $C(^3P)$ + H^+. Experiments measuring the absolute cross sections for electron impact dissociation of CH^+ ions producing C^+ ions were reported by Bannister *et al* (2003). Figure 3 shows the results of Bannister *et al* (2003) together with our theoretical results for the dissociation to the asymptotic states $C^+(^2P)$ + $H(^2S)$ (thick curve), $C(^3P)$ + H^+ (thin curve) and their sum (topmost curve). Our results were calculated with the assumption that all excitations from the X $^1\Sigma^+$ ground state to the states, dissociating to a particular asymptote, above the corresponding dissociation threshold result in dissociation. Even at these energies, however, such excitation cross sections would include both dissociation and electronic excitation cross sections, as electronic excitation to the core excited bound states competes with dissociation. The contribution of cross sections corresponding to 'pure' electronic excitation were estimated using Franck-Condon factors and these were then subtracted out to get the dissociation cross sections.

Our results agree reasonably well with the measurements of Bannister *et al* (2003) from the threshold (10 eV) to about 18 eV and are within 20% of the measured values. Above this we would expect our results underestimate the cross section due to neglect of higher lying states which were not included in our calculations. However, the appearance of agreement of the summed cross section (top most curve in Figure 3) may be largely coincidental. The experiments were performed on a hot sample of CH^+ whose state distribution was not determined. This leads to significant measured cross sections from below threshold to dissociation for the X $^1\Sigma^+(\nu = 0)$ ground state. This may well be due to the presence of a significant population of CH^+ ions in their a $^3\Pi$ metastable state (Bannister *et al* 2003). Without knowledge of the experimental state distribution

it is not possible to make a proper comparison with our results.

4. Conclusions

In this paper we report *R*-matrix calculations on electron collision with CH^+. An initial CI calculation was done for the CH^+ target states, which were then used in a scattering calculation to yield bound and resonant states of CH at a single geometry. The CH bound states agreed well with earlier calculations. We have also calculated cross sections for vibrationally resolved electron impact excitation, and electron impact dissociation of CH^+ ions. Our electron impact dissociation cross sections are in reasonable agreement with the only available experimental measurement and do not deviate from the experimental values by more than 20%. However, given the experimental conditions it is not clear if this represents a like-for-like comparison. To the best of our knowledge, this is the only available *ab initio* theoretical calculation of the dissociation process.

5. Supplementary data

The vibrationally resolved electronic excitation and dissociation cross sections presented in this work are available in electronic form as supplementary data.

6. Acknowledgements

We are deeply indebted to Robert Le Roy for helping us with his LEVEL16 program used to calculate the Franck-Condon factors used in this work. RG gratefully acknowledges CSIR, New Delhi, for a Junior Research Fellowship. We also thank Ioan Schneider for numerous discussions on the CH^+/CH states.

References

Amitay Z, Zajfman D, Forck P, Hechtfischer U, Seidel B, Grieser M, Habs D, Repnow R, Schwalm D and Wolf A 1996 *Phys. Rev. A* **54**, 4032

Bannister M E Krause H F, Vane C R, Djurić N, Popović D B, Stepanović M, Dunn G H, Chung Y S, Smith A C H and Wallbank B 2003 *Phys. Rev. A* **68**, 042714

Barnett A R 1982 *Computer Phys. Comms.* **27**, 147–166

Barinvos G and van Hemert M C 2004 *Chem. Phys. Lett.* **399**, 406–411

Biglari Z, Shayesteh A, Maghari A 2014 *Comput. Theoret. Chem.* **1047**, 22–29

Boukaline F, Grozdanov T P, Andric L and McCaroll R 2005 *J. Chem. Phys.* **122**, 044108

Burke P G 2011 *R-Matrix Theory of Atomic Collisions* (Springer, Heidelberg) .

Buttle P J A 1967 *Phys. Rev.* **160**, 719–29

Cade P E and Huo W M, 1967 *J. Chem. Phys.* **47**, 614–648

Carata L, Orel A E, Raoult M, Schneider I F and Suzor-Weiner A 2000 *Phys. Rev. A* **62**, 052711

Chakrabarti K & Tennyson J 2012 *Eur. Phys. J.* D **66**, 31

Cho Y S & Le Roy R J 2016 *J. Chem. Phys.* **144**, 024311

Douglas A E and Herzberg G 1941 *Astrophys. J.* **94**, 381

Douglas A E and Herzberg G 1941 *Canadian. J. Res.* **20**, Sec A, 71
Faure A, Halvick P, Stoecklin T, Honvault P, Epee Epee M D, Mezei J Zs, Motapon O, Schneider I F, Tennyson J, Roncero O, Bulut N and Zanche A 2017 *Mon. Not. R. astr. Soc.* in press.
Godard B, Falgarone E, Gerin M, Lis D C, De Luca M, Black J H, Goicoechea J R, Cernicharo J, Neufeld D A, Menten K M and Emprechtinger M 2012 *Astron. Astrophys.* **540**, A87
Godard B and Cernicharo J 2013 *Astron. Astrophys.* **550**, A8
Hakalla R, Kepa R, Szajna W and Zachwieja M 2006 *Eur. Phys. J. D* **38**,481
Hamilton J R, Faure A and, Tennyson J 2016 *Mon. Not. R. Astron. Soc.* **455**, 3281
Hayden Smith Wm, Liszt H S and Lutz B L 1973 *Astrophys. J.* **183**, 69–80
Herzberg G and, Johns J W C 1969 *Astrophysics J.* **158**,399
Kanzler A W Sun H and Freed K F 1991 *Int. J. Quant. Chem.* **XXXIX**, 269–286
Kowalski K and Piecuch P 2001 *Chem. Phys. Lett.* **347**, 237–246
Laporta V, Chakrabarti K, Celiberto R, Janev R K, Mezei J Zs, Niyonzima S, Tennyson J & Schneider I F 2017 *Plasma Phys. Control. Fusion*, **59**, 045008
Le Roy R J 2017 *J. Quant. Spectrosc. Radiat. Transf.* **186**, 167 - 178.
Lim A J, Rabadán I and Tennyson J 1999 *Mon. Not. R. Astron. Soc.* **306**, 473–478
Liszt H S & Hayden Smith Wm 1972 *J. Quant. Spectrosc. Radiat. Transfer.*, **412**, 947
Little D A, Chakrabarti K, Mezei J Zs, Schneider I F & Tennyson J 2014 *Phys. Rev. A*, **90**, 052705
Lorquet A J, Lorquet J C, Wankenne H, Momigny J & Lefebvre-Brion H 1971 *J. Chem. Phys*, **55**, 4053
Mezei J Zs, Colboc F, Pop N, Ilie S, Chakrabarti K, Niyonzima S, Lepers M, Bultel A, Dulieu O, Motapon O, Tennyson J,Hassouni K and Schneider I F 2016 *Plasma Sources Sci. Technol.* **25**, 055022
Morgan L A 1984 *Comput. Phys. Commun.* **31**, 419.
Morgan L A, Tennyson J & Gillan C J 1998 *Computer Phys. Commun.* **114**, 120–128.
Myers A T, McKee C F, Li P S 2015 *Mon. Not. R. Astron. Soc.* **453**, 2747
Nagy Z, Van der Tak F F S, Ossenkopf V, Gerin M, Le Petit F, Le Bourlot J, Black J H, Goicoechea J R, Joblin C, Rllig M and Bergin E A 2013 *Astron. Astrophys.* **550**, A96
Noble C J & Nesbet R K 1984 *Computer Phys. Comms.* **33**, 399–411
Rabadán I & Tennyson J 1996 *J. Phys. B: At. Mol. Opt. Phys.* **29**, 3747-3761
Rabadán I & Tennyson J 1997 *J. Phys. B: At. Mol. Opt. Phys.* **30**, 1975-1988
Sarpal B K, Branchett S E, Tennyson J & Morgan L A 1991 *J. Phys. B: At. Mol. Opt. Phys.* **24**, 3685–3699.
Sauer S P A & Špirko 2013 *J. Chem. Phys.* **138**, 024315
Song C, Han H, Zhang Y, Yu Y and Gao T 2008 *Can. J. Phys.* **86**, 1145–1151
Tawara H, in *Atomic and Molecular Processes in Fusion Plasmas*, edited by R. K. Janev Plenum, New York, 1995, pp. 461-496.
Tennyson J 1988 *J. Phys. B: At. Mol. Opt. Phys.*, **21**,'805-816.
Tennyson J & Morgan L A 1999 *Phil. Trans. Royal Soc. London A* **357**, 1161–1173
Tennyson J and Noble C J 1984 *Comput. Phys. Commun.* **33**, 421–424
Tennyson J 1988 *J. Phys. B: At. Mol. Opt. Phys.* **21**, 805–816
Tennyson J 2010 *Phys. Rep.* **491**, 29-76.
van Dishoeck E F 1987 *J. Chem. Phys.* **86**, 196–214
Zhang R, Baluja K L, Franz J & Tennyson J 2011 *J. Phys. B: At. Mol. Opt. Phys.* **44**, 035203